# How Online Social Ties Influence the Epidemic Spreading of a Multiplex Network?

Xianzhe Tang, Yuan Zhang, Cong Li*, Xiang Li
*Adaptive Networks and Control Lab, Department of Electronic Engineering, Fudan University*
*Research Center of Smart Networks and Systems, School of Information Science and Engineering, Fudan University*
*MOE Frontiers Center for Brain Science, Institutes of Brain Science, Fudan University*
Shanghai, China
{17210720150, 17210720049, cong_li, lix}@fudan.edu.cn

***Abstract*—In recent years, many studies have focused on the interrelation between the epidemic spreading and the spread of awareness to prevent infections. A multiplex network is utilized to depict this scenario. The upper layer of the multiplex network represents an online social network, where the awareness of epidemic spreads. The lower layer of the multiplex network represents an off-line social network, where the epidemic spreads among individuals. However, most previous studies neglected that the online social network has diverse social ties, such as the dense social ties (in-roles and friends) and the sparse social ties (familiar strangers and strangers). In this work, we study how the online social ties impact on epidemic spreading in the off-line social network. We assume that besides the same dense in-roles and friends, an online social network could have only familiar strangers, only strangers, or both. We analyze the influence of the effective epidemic spreading rate and the awareness spreading rate on the infection fraction at the steady state with two empirical datasets. An interesting finding is that an online social network containing strangers is more likely to reduce epidemic prevalence than that containing familiar strangers.**

## I. INTRODUCTION

Epidemic spreading in social networks has a great impact on our lives, and has been studied for a long time. Many mathematical models [1] [2] [3] [4] [5] have been proposed to describe the spread of infectious virus, and the most classical epidemic spreading model is the compartmental model. The susceptible-infected-susceptible (SIS) model is one of the most studied compartment models and has two compartments: susceptible (S) and infected (I). An infected individual (I) infects its susceptible (S) neighbors (direct contact) with an infection probability $\beta$, and recovers with a probability $\mu$. The effective spreading rate is defined as $\lambda = \frac{\beta}{\mu}$. Epidemic threshold $\beta_c$ is a critical point of effective spreading rate which separates two phases of epidemic spreading processes: If $\beta < \beta_c$, the infection dies out and the the infection fraction at the steady state $\rho_I = 0$; If $\beta > \beta_c$, the infection will become pandemic and $\rho_I$ will approach a stable value.

The spread of awareness always accompanies the epidemic spreading. Wang *et al.* [6] analyzed the influenza-like illness dataset and the Google Flu Trends dataset, found that epidemic spreading promotes awareness spreading, but awareness spreading suppresses epidemic spreading. In other words, there are asymmetric interactions between the awareness spreading and virus spreading. Funk *et al.* [7] introduced the spread of awareness into an epidemiological model. They found that the awareness could reduce the infection fraction $\rho_I$, but does not affect the epidemic threshold $\beta_c$. To keep things simple, many studies focused on the interplay between epidemic spreading and awareness spreading in static networks [8] [9] [10]. Granell *et al.* [11] studied the interplay between epidemic spreading and awareness spreading in multiplex networks. They built a multiplex network with two layers: the upper layer represents an online social network, and the lower layer represents an off-line social network. They found that the epidemic threshold $\beta_c$ is determined by the awareness dynamics and the topology of the online social network. Guo *et al.* [12] assumed that the information spreading layer is a time-varying network which is generated by the activity-driven model [13]. They found that the awareness spreading cloud increase the epidemic threshold $\beta_c$ and reduce the epidemic prevalence.

Besides the awareness spreading, social ties in social networks have a great influence on epidemic spreading. Social ties are regarded as the connections among individuals. Individuals share information through social ties in the online social networks, and have face-to-face contacts through social ties in the off-line social networks. Social ties consist of strong social ties (in-roles and friends) and weak social ties (familiar strangers and strangers) [14]. Granovetter [15] created the "strength of weak ties" hypothesis, that people are more likely to get a job through weak ties rather than strong ties. The debate on which social ties are more important continues to this day. Previous studies [16] [17] have shown that strong ties construct community structures in the network, and weak ties create bridges between them. Karsai *et al.* [18] defined the strength of social tie as the total number of calls between two individuals, and observed that strong ties severely suppress the information spreading by creating recurrent interaction patterns. Refs. [19] [20] suggest that strong ties play a more important role than weak ties in the process of art creating. Wu *et al.* [21] investigated a face-to-face interactions network, and found that teams mainly consisting of strong ties are more efficient than teams mainly consisting of weak ties when executing complex tasks. They have given an explanation that strong ties could build up an information-rich communication

ISBN 978-3-903176-28-7 © 2020 IFIP

media for transferring the complex knowledge.

The impact of awareness spreading on epidemics and the role of social ties in spreading processes has been discussed. So far, the influence of the social ties in the awareness spreading networks on the epidemic process has scarcely been discussed. In this work, we generate several online social networks which contain different social ties, and find out the influence of the social ties on epidemic spreading of an online-offline mulitplex network. This work is organized as follows. In Section II, we introduce methods for identifying social ties in social networks, and build an online-offline mulitplex network model with two layers: the online social network and the off-line social network. In Section III, we introduce the UAU-SIS dynamics. In our online-offline mulitplex network model, the epidemic spreads on the off-line social network and the awareness of epidemic spreads on the online social network. Two spreading processes interact with each other. In Section IV, we introduce two empirical campus Wi-Fi datasets and construct online-offline mulitplex networks with them. Then we analyze the characteristics of each type of social tie in the constructed networks. In Section V, We analyze the influence of the social ties in online social networks on the epidemic spreading with the online-offline mulitplex networks. We observe that the online social network containing strangers leads to a smaller infection fraction than that containing familiar strangers. Finally, we conclude in Section VI.

## II. Network model

### A. Social ties in the network

Most previous studies divide social ties into two types: the strong ties and the weak ties. For instance, Karsai *et al.* [18] analyzed a mobile phone call dataset and separated social ties into strong and weak ties by the number of calls between individuals. However, social ties in social networks are diverse. The familiar stranger is a kind of social ties, that individuals could recognize each other but never interact. Milgram [22] first proposed the concept in 1972 through a famous subway experiment. He took a photo for the passengers at a subway station. One week later, he distributed the photo to the passengers at the same subway station and the same time, and let them find out whether any person in the photo looks familiar. The result is that up to 89% of respondents identified at least one impressed stranger in the photo. Paulos *et al.* [23] reproduced this experiment thirty years later to find the impact of the widely use of mobile phone on the identification of familiar strangers. As the result, 78% of respondents identified at least one impressed stranger. Although the ratio 78% is lower than Milgram's experimental, the result shows that familiar strangers are still common in daily lives. Sun *et al.* [24] analyzed the travel smart card data in Singapore. They defined the familiar strangers as passengers who were on the same bus at the same time, and believed that the familiar strangers are caused by the limit of encounters, which is brought by individual's regular activities. In this work, we divide social ties into four types: in-roles (such as colleagues and classmates) [25], friends, familiar strangers and strangers, with the social tie classifier proposed in [14]. The first two are dense social ties (strong ties) and the second two are spare social ties (weak ties). A time-varying off-line social network with edge set $E$ can be divided in to $N$ cycles with individuals' behavioral periodicity $T$. Individuals' behaviors are represented by a behavioral matrix $S_n(u) = [s_{t,l}^{u,n}]$, where $u$ is the individual index, $n$ represents the $n$-th cycle, $t \in [1, T/\Delta T]$ ($\Delta T$ is the time step length of the time-varying network) is the time step and $l \in [1, |L|]$ ($|L|$ is the number of interaction locations) is the location index. If individual $u$ visits location $l$ at time step $t$ of the $n$-th cycle, $s_{t,l}^{u,n} = 1$, otherwise $s_{t,l}^{u,n} = 0$. The interaction weight $w_{t,l}^{u,v}$ and the interaction probability $prob_{t,l}^{u,v}$, between two individuals $u$ and $v$, are calculated as follows:

$$w_{t,l}^{u,v} = |\{n|(u,v,t,l,n) \in E, n = 1 \cdots N\}|, \tag{1}$$

$$prob_{t,l}^{u,v} = \frac{\sum_{n=1}^{N} s_{t,l}^{u,n} \times \sum_{n=1}^{N} s_{t,l}^{v,n}}{N^2}. \tag{2}$$

Next, we calculate two metrics, the encounter regularity $d_r$ and the spatiotemporal entropy $d_e$. The encounter regularity $d_r$ which measures to what degree the interactions between a pair of individuals $u$ and $v$ is generated obeying the periodic life routines,

$$d_r(u,v) = \frac{\sum_t \sum_l (w_{t,l}^{u,v} \times prob_{t,l}^{u,v})}{\sum_t \sum_l w_{t,l}^{u,v}}, \tag{3}$$

and the spatiotemporal entropy $d_e$ measures the degree of social similarity,

$$d_e(u,v) = \log_2 \sum_t \sum_l sign(w_{t,l}^{u,v}). \tag{4}$$

Four types of social ties are identified based on these two metrics. We first generate a null model by degree-preserving rewiring [26] links in the origin time-varying network (details see [14]). Then, we let the complementary cumulative distribution functions of the null model $P(d_r^{null}(u,v) > r_0) = P(d_e^{null}(u,v) > e_0) = p_0 = 10^{-3}$, to get the critical thresholds $r_0$ and $e_0$ of $d_r$ and $d_e$. Social ties are classified as follows,

- if $d_r(u,v) > r_0$ and $d_e(u,v) > e_0$, $u$ and $v$ are in-roles,
- if $d_r(u,v) < r_0$ and $d_e(u,v) > e_0$, $u$ and $v$ are friends,
- if $d_r(u,v) > r_0$ and $d_e(u,v) < e_0$, $u$ and $v$ are familiar strangers,
- otherwise, $u$ and $v$ are strangers.

For the sake of brevity, we denote in-roles and friends, which are both dense social ties, by F&IR, the familiar strangers by FS, and the strangers by S. Note that the social ties of individuals who only interact with each other once belong to S by definition in [14], which is not considered in this work.

### B. Online-offline mutiplex network model

The time-aggregated representation of the off-line social network contains all social ties between individuals, and we divide them into four types of social ties, *i.e.* in-roles (IR), friends (F), familiar strangers (FS) and strangers (S), by the

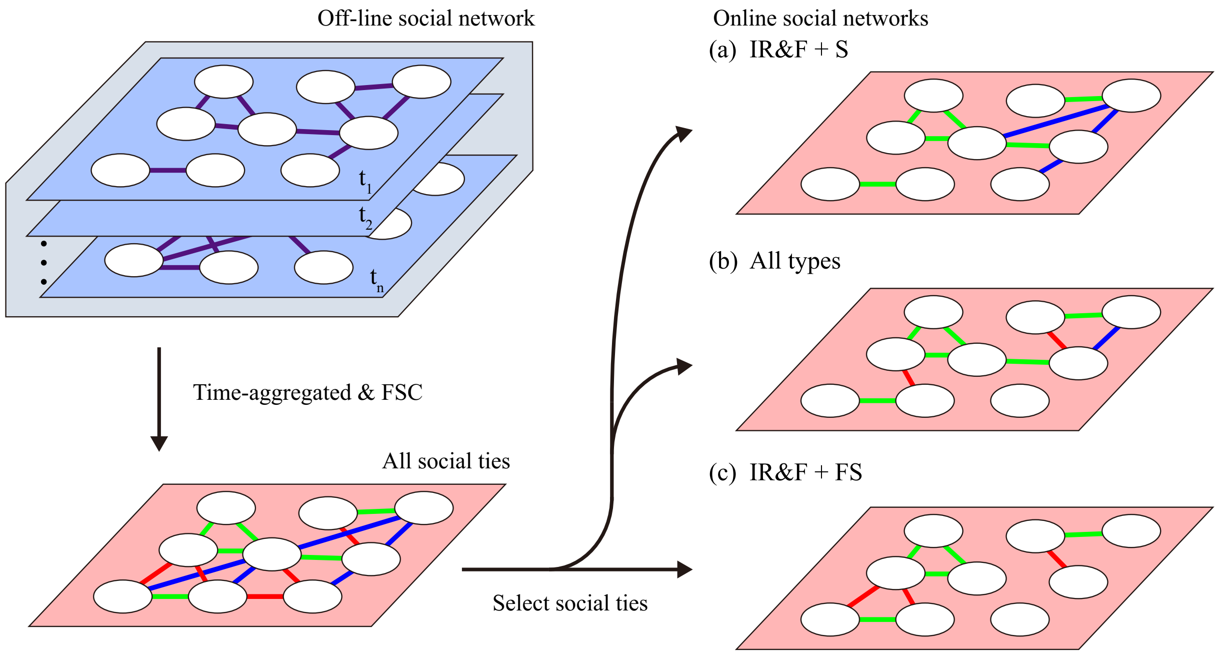


Fig. 1. The generating process of the three online social networks. (a) IR&F+S, consists of in-roles, friends and strangers; (b) All types, consists of all four types of social ties; (c) IR&F+FS, consists of in-roles, friends and familiar strangers. IR&F, green lines; FS ,red lines; and S, blue lines. All the social ties are identified on the time-varying off-line social network. All online social networks have the same number of edges, and the sets of IR&F edges are the same.

social tie classifier [14] that we introduced in Section II A. IR&F belongs to dense social ties, which has higher interaction frequency than FS and S. In real life, individuals are more likely to build a friendship in the online social network with IR&F. Meanwhile, individuals could build a friendship in the online social network with the sparse social ties, i.e. FS and S, via the friend recommendation systems provided by social media platforms, such as "People You May Know" or "People Nearby". Refs. [24] [14] have found that the average number of FS and S is much lager than IR&F, indicating that sparse social ties in online social networks might play an important role and should not be ignored. In order to figure out the impact of the social ties in the online social network on epidemic spreading, here we generate three online social networks containing different types of social ties:

1) Only contains IR&F and S (IR&F+S);
2) Contains all four types of social ties (All types);
3) Only contains IR&F and FS (IR&F+FS).

We here guarantee that the three online social networks have the same number of edges and the same set of IR&F edges. For the IR&F+FS online social network, we select the FS edges randomly with uniform probability $\eta$. Other online social networks are generated by taking the same number of edges as the IR&F+FS. That means, for the All types online social network, the FS and S edges are randomly selected with uniform probability $\eta\frac{|FS|}{|FS|+|S|}$, and for the IR&F+S online social network, the S edges are randomly selected with uniform probability $\eta\frac{|FS|}{|S|}$. The online social networks generating process is shown in Fig.1.

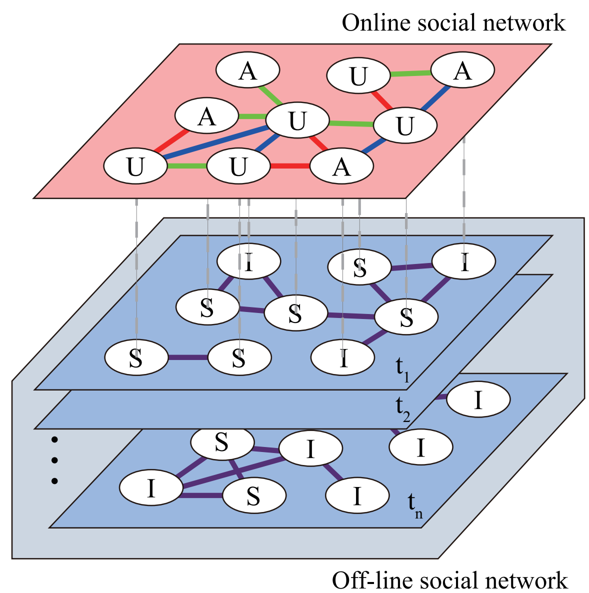


Fig. 2. The structure of multiplex networks. The upper layer is a static online social network, where individuals are aware (A) or unaware (U) in the process of awareness spreading. The lower layer is a time-varying off-line social network. The individuals are the same as that in the online social network, and they cloud be susceptible (S) or infected (I) in the process of epidemic spreading.

## III. UAU-SIS DYNAMICS

In this work, we study the awareness spreading and epidemic spreading with the Unaware-Aware-Unaware-Susceptible-Infected-Susceptible (UAU-SIS) model [11] [27] on a multiplex network with two layers. A two-layer multiplex network with different network topologies is illustrated in Fig.2. The upper layer is a static online social network, where the awareness spreads and the lower layer is a time-varying off-line social network, where the epidemic spreads. The off-line social network consists of all contacts among in-roles, friends, familiar strangers and strangers. Meanwhile, individuals are likely to establish online contacts with who they have met off-line. That is to say, the online social network may comprise part of the contacts in off-line social network.

In the online social network, awareness spreads in a cyclic process satisfying the cycle unaware-aware-unaware (UAU). Individuals have two states: unaware (U) and aware (A). Unaware individuals are those who do not know or have forgotten the information of epidemics, and do not take measures to prevent the infection. The awareness is generated in two ways: an unaware individual is informed by aware neighbors with a probability $\nu$, or the individual obtains the awareness along with being infected. Aware individuals forget or no longer care about the epidemics with a probability $\delta$, and become unaware again. In the off-line social network, an SIS spreading process takes place among the individuals. We denote the unaware infection probability by $\beta^U$. However, the risk to be infected is lower for aware individuals than unaware individuals. The infection probability $\beta^A$ for aware individuals is reduced by a factor $\gamma$, *i.e.* $\beta^A = \gamma\beta^U$. Once an individual is infected, it is immediately aware of epidemics and changes the state in the online social network, tries to arouse the neighbors' attention. The recovery rate for all infected individuals is the same $\mu$. The whole scheme is shown in Fig.3. The individuals can be in three states: unaware and susceptible (US), aware and susceptible (AS), aware and infected (AI). Let us denote the elements of adjacency matrices of the online social network and the snapshot of off-line social network at time $t$ by $a_{ij}$ and $b_{ij}$, respectively. If there is a contact between individuals i and j in the online (or offline) social network, $a_{ij} = 1$ (or $b_{ij} = 1$), otherwise $a_{ij} = 0$ (or $b_{ij} = 0$). Each individual $i$ has a certain probability of being in one of the three states at time $t$, denoted by $p_i^{US}(t)$, $p_i^{AS}(t)$ and $p_i^{AI}(t)$, respectively. The transition probabilities $r_i(t)$ for individual $i$ not being informed by any neighbors, the probability $q_i^A(t)$ for an aware individual not being infected by any neighbors, and the probability $q_i^U(t)$ for an unaware individual not being infected by any neighbors are

$$\begin{aligned} r_i(t) &= \prod_j \{1 - a_{ij}[p_j^{AS}(t) + p_j^{AI}(t)]\nu\}, \\ q_i^A(t) &= \prod_j [1 - b_{ij}(t) p_j^{AI}(t)\beta^A], \\ q_i^U(t) &= \prod_j [1 - b_{ij}(t) p_j^{AI}(t)\beta^U], \end{aligned} \tag{5}$$

respectively. Hence, we obtain the equations of states transfer probabilities in the UAU-SIS dynamics

$$\begin{aligned} p_i^{US}(t+1) =& p_i^{AI}(t)\mu\delta + p_i^{US}(t) r_i(t) q_i^U(t) + p_i^{AS}(t)\delta q_i^U(t), \\ p_i^{AS}(t+1) =& p_i^{AI}(t)\mu(1-\delta) + p_i^{US}(t)[1 - r_i(t)] q_i^A(t) \\ &+ p_i^{AS}(t)(1-\delta) q_i^A(t), \\ p_i^{AI}(t+1) =& p_i^{AI}(t)(1-\mu) + p_i^{US}(t)\{[1 - r_i(t)][1 - q_i^A(t)] \\ &+ r_i(t)[1 - q_i^U(t)]\} + p_i^{AS}(t)\{\delta[1 - q_i^U] \\ &+ (1-\delta)[1 - q_i^A(t)]\}. \end{aligned} \tag{6}$$

We then compare the UAU-SIS dynamics under the three different online-offline multiplex social networks.

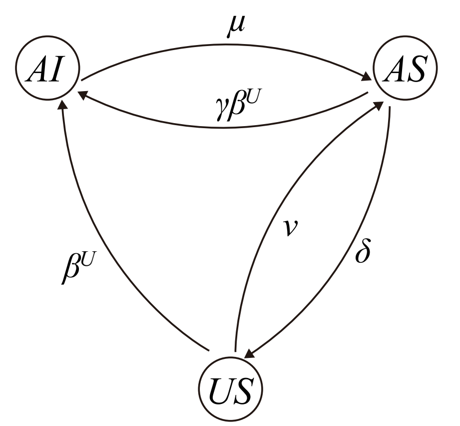


Fig. 3. Transition probabilities between unaware and susceptible (US), aware and susceptible (AS), as well as aware and infected (AI), in UAU-SIS dynamic for each time step. The $\beta^U$ is the unaware infection probability. The $\gamma\beta^U$ is the aware infection probability. The $\mu$ is the probability of recovery. The $\nu$ is the transition probability from unaware to aware. The $\delta$ is the transition probability from aware to unaware.

## IV. Empirical Analysis

Two empirical datasets used in this work are both campus Wi-Fi datasets, one is collected in Chinese campus (FDU13 [28]) and the other is collected in American campus (USC06 [29]). The Wi-Fi datasets record the logs of accessing to wireless access points (WAP) that are distributed in Fudan University and University of Southern California, respectively. All of the logs in each dataset have the same format $(u, t, \Delta t, l)$, where $u$ represents the individual $u$ who accesses to Wi-Fi, the $t$ represents the beginning time of the $u$'s accessing to WAP, the $\Delta t$ represents the duration of the accessing and $l$ represents the location of the WAP. The details of the datasets are shown in Table I.

We convert the campus Wi-Fi datasets into the off-line social networks. If two individuals $u$ and $v$ accessed the same WAP at the same time, we assume that an interaction happened between them, based on the geographic coincidence [30]. This assumption may induce inaccuracies, but the reasonableness has been supported by many previous studies [14] [31] [32] [33]. In order to better represent the interactions between individuals, we discretize the whole observation time $NT$ with $\Delta T$-long step, where $\Delta T$ depends on the scenario depicted in

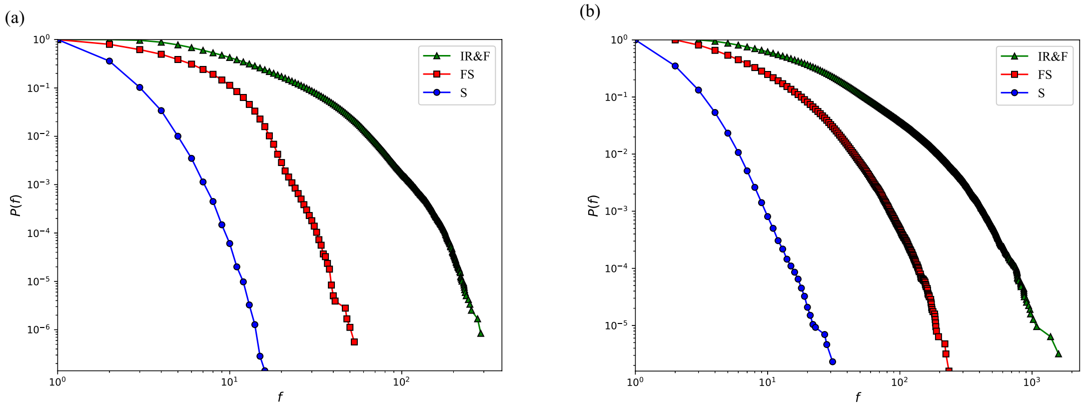


Fig. 4. The complementary cumulative distribution functions (CCDFs) of interaction frequencies for each type of social tie in (a) FDU13 dataset and in (b) USC06 dataset.

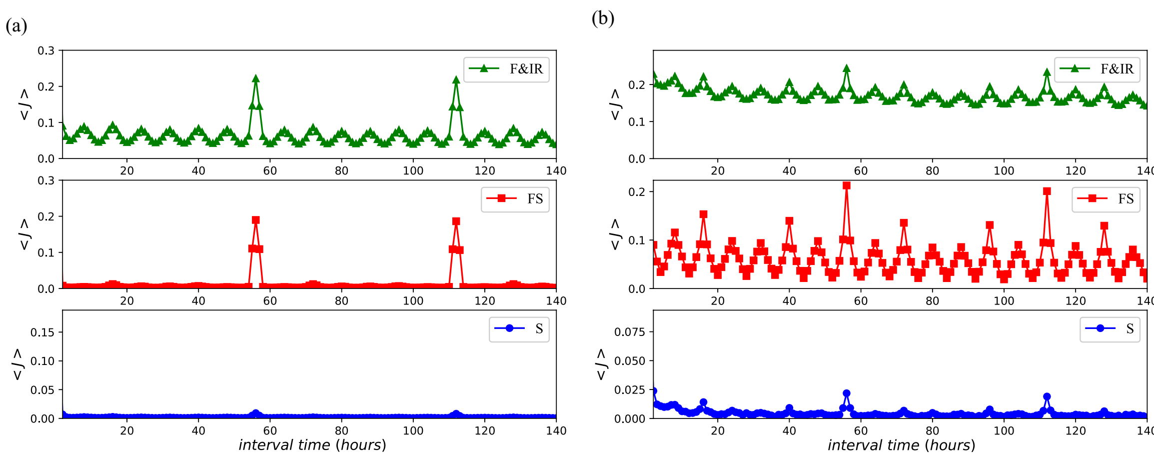


Fig. 5. The average Jaccard's coefficient versus interval time for each type of social tie in (a) FDU13 dataset and in (b) USC06 dataset.

TABLE I
STATISTICAL INFORMATION OF TWO EMPIRICAL DATASETS. NOTATIONS ARE THE NUMBER OF INDIVIDUALS $|U|$, THE NUMBER OF LOCATIONS $|L|$, THE NUMBER OF RECORDS $R$, THE NUMBER OF CYCLES $N$ AND THE INDIVIDUAL BEHAVIOR PERIODICITY $T$ (DAYS).

| Dataset | $\|U\|$ | $\|L\|$ | $R$ | $N$ | $T$ |
|---|---|---|---|---|---|
| FDU13 | 10146 | 1452 | 3825382 | 12 | 7 |
| USC06 | 5185 | 137 | 808015 | 84 | 1 |

TABLE II
PERCENTAGE OF EACH TYPE OF SOCIAL TIE IN TWO DATASETS.

| Dataset | IR | F | FS | S |
|---|---|---|---|---|
| FDU13 | 4.4% | 1.7% | 40.1% | 53.8% |
| USC06 | 15.6% | 1.8% | 34.8% | 47.8% |

the dataset [33]. If $\Delta T$ is too large, the coarse granularity will result in loss of temporal information. While a too small $\Delta T$ introduces a lot of disturbance noise into the off-line social network. Empirically, we set $\Delta T = 3$ hours for FDU13 and USC06 datasets, which is the representative time variance of behaviors in daytime of individuals from one day to the next [34]. A time-varying off-line social network with $NT/\Delta T$ time steps is built. If two individuals have an interaction at time $t$, an edge is add into the snapshot of time step $\lceil t/\Delta T \rceil$.

Then, we identify the social ties by applying the social tie classifier [14] to the off-line social networks. Here the critical thresholds $(r_0, e_0)$ generated by null models are (0.098, 2.152) for FDU13 dataset and (0.002, 1.585) for USC06 dataset. The social ties classification results of two empirical datasets are shown in Table II. In all datasets, the percentage of S is the largest among the four types, and the percentage of FS surpasses that of IR&F greatly.

We further analyze the characteristics of each type of social tie. The interaction frequency $f$ measures the total number of interactions between two individuals in off-line social networks [18]. Fig.4 shows the complementary cumulative distribution functions (CCDFs) $P(f)$ of interaction frequencies for each type of social tie. In all datasets, IR&F contributes the highest interaction frequency because of the close contacts among classmates in the campus environment. The $P(f)$ of S follows the narrowest interaction frequency

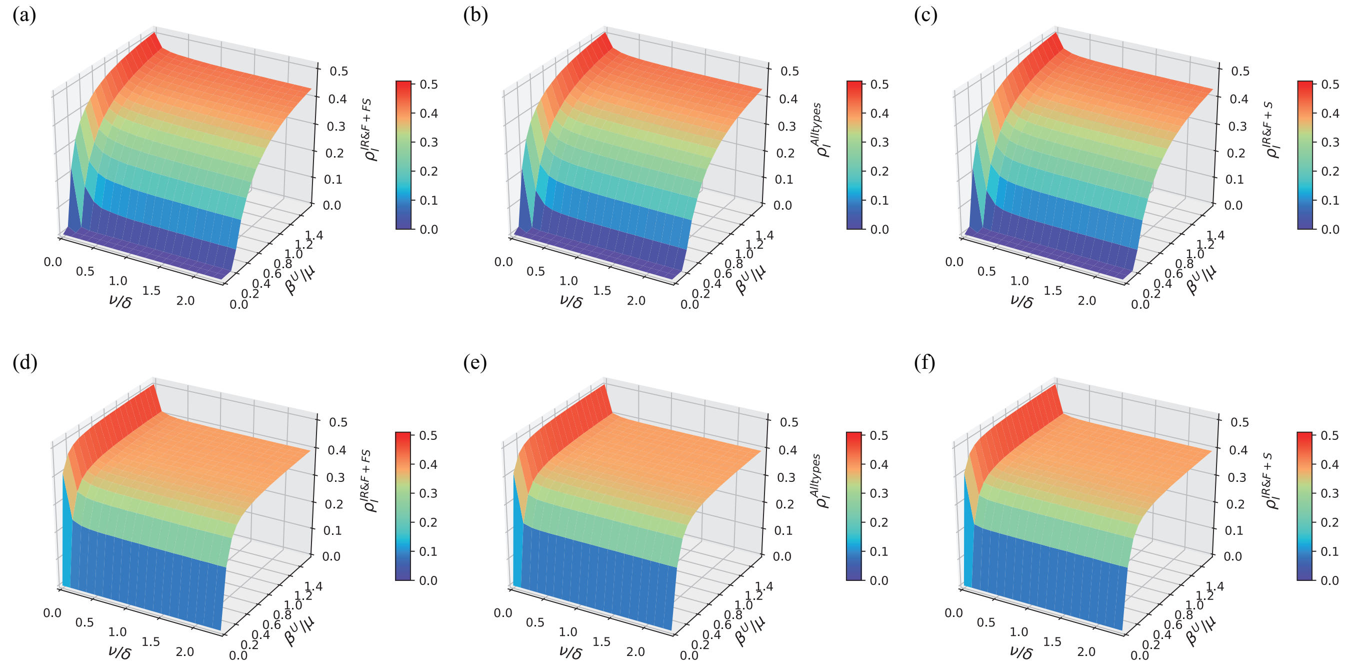


Fig. 6. The density of infected individuals at the steady state $\rho_I$ versus the effective epidemic spreading rate $\beta^U/\mu$ and the awareness spreading rate $\nu/\delta$ in UAU-SIS dynamics with different online-offline multiplex networks. (a), (b), (c) are simulated with FDU13; (d), (e), (f) are simulated with USC06. (a), (d) have the online social network IR&F+FS; (b), (e) have the online social network All types; (c), (f) have the online social network IR&F+S.

distribution due to the completely random interactions between strangers. In particular, the interaction frequency of FS is medium between that of IR&F and S. The Jaccard's coefficient [35], which characterizes the similarity between neighbors of two individuals, is defined as the size of the intersection of the neighbors of two individuals, $\Gamma(u)$ and $\Gamma(v)$, divided by the size of their union,

$$J(u,v) = \frac{|\Gamma(u) \cap \Gamma(v)|}{|\Gamma(u) \cup \Gamma(v)|}. \tag{7}$$

For each individual $u$, we calculate the intersection of the neighbors of $u$ at time $t$ and $t+\tau$ ( where $t \in [1, T/\Delta T - \tau]$), $\Gamma(u,t)$ and $\Gamma(u,t+\tau)$, divided by the size of their union,

$$J(u,\tau) = \frac{|\Gamma(u,t) \cap \Gamma(u,t+\tau)|}{|\Gamma(u,t) \cup \Gamma(u,t+\tau)|}. \tag{8}$$

Then we get the average Jaccard's coefficient of all individuals on intervals $\langle J \rangle(\tau)$, which quantify the repeatability of interactions. Fig.5 shows the average Jaccard's coefficient versus interval time for each type of social tie. In all datasets, the average Jaccard's coefficient $\langle J \rangle$ of IR&F and FS have prominent peaks at multiples of cycle length $T$, indicating a strong periodicity in repeated interactions between the individuals with that social ties. The periodicity should be caused by the weekly course schedules. Because of the completely random interactions, the average Jaccard's coefficient $\langle J \rangle$ of S is low.

## V. Simulations

In this work, we fix $\gamma = 0$, which means that susceptible individuals are completely protected from the infection when they get awareness of the epidemic. For instance, aware individuals will practice self-quarantine. The initial fraction of infected individuals is 0.001 (10 for FDU13 and 5 for USC06). All results are averaged over 1000 realizations.

We first investigate the influence of the effective epidemic spreading rate $\beta^U/\mu$ and the awareness spreading rate $\nu/\delta$ on the stationary density of infected individuals $\rho_I$ in UAU-SIS dynamics with the online-offline multiplex social networks. We here fix the edge selection probability $\eta = 0.3$, $\mu = 0.4$, $\delta = 0.6$. The range of the effective epidemic spreading rate $\beta^U/\mu$ is [0, 2.5] (infection probability $\beta^U \in [0,1]$) and the range of the awareness spreading rate $\nu/\delta$ is [0, 1.66] (transition probability from unaware to aware $\nu \in [0,1]$). Fig.6 shows that the epidemic prevalence $\rho_I$ increases with the effective epidemic spreading rate $\beta^U/\mu$ and decreases with the awareness spreading rate $\nu/\delta$, regardless of the dataset and the social ties in online social network.

We find that the stationary density of infected individuals $\rho_i$ increases with the increase of effective spreading rate in multiplex networks from USC06 much faster than that in multiplex networks from FDU13. For instance, when $\beta^u/\mu = 0.6$, the stationary density of infected individuals $\rho_i$ in multiplex networks from USC06 is already close to 0.4, however, the $\rho_i$ in multiplex networks from FDU13 is around 0.2. When the effective spreading rate is large enough, the stationary density of infected individuals $\rho_i$ increases slowly. Moreover, we find that the epidemic threshold in multiplex networks from USC06 is much smaller than that in multiplex networks from FDU13. The phenomena might be caused by the higher repetitions of the same interactions in USC06 than that in FDU13, which we found in Section IV. As shown in Fig.5, the

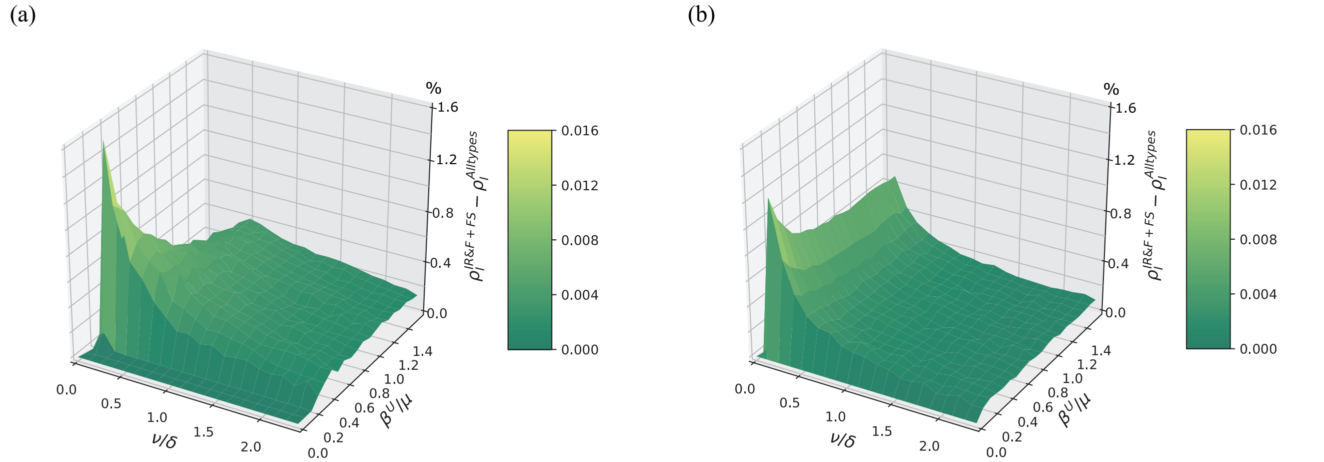


Fig. 7. The difference $\rho_I^{IR\&F+FS} - \rho_I^{Alltypes}$ between the stationary density of infected individuals in multiplex networks with online social network IR&F+FS and that with online social network All types versus the effective epidemic spreading rate $\beta^U/\mu$ and the awareness spreading rate $\nu/\delta$ in UAU-SIS dynamics with (a) FDU13 dataset and (b) USC06 dataset.

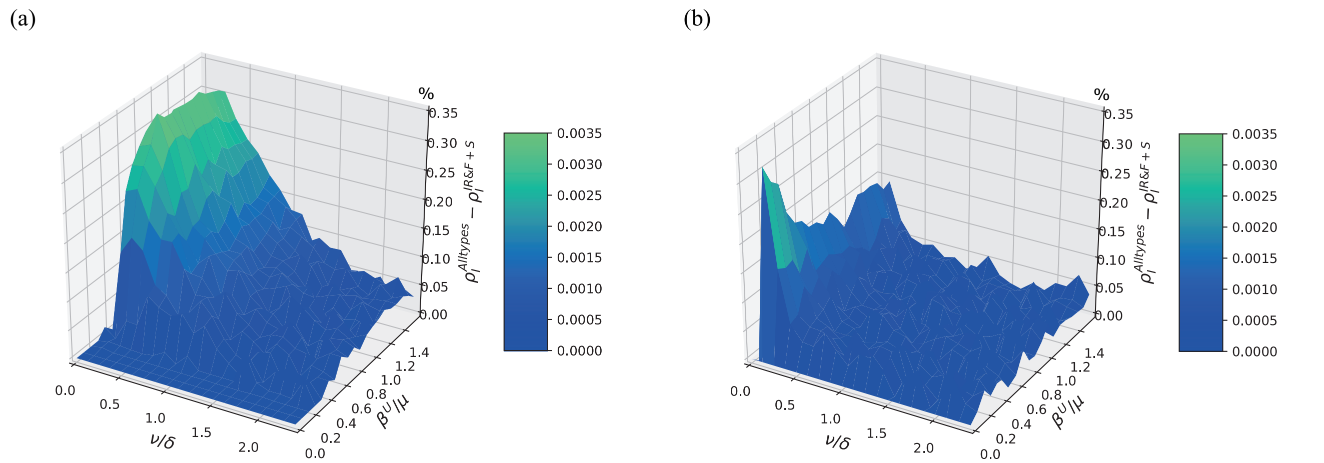


Fig. 8. The difference $\rho_I^{Alltypes} - \rho_I^{IR\&F+S}$ between the stationary density of infected individuals in multiplex networks with online social network All types and that with online social network IR&F+FS versus the effective epidemic spreading rate $\beta^U/\mu$ and the awareness spreading rate $\nu/\delta$ in UAU-SIS dynamics with (a) FDU13 dataset and (b) USC06 dataset.

average Jaccard's coefficient $\langle J \rangle$ in USC06 is larger than that in FDU13, which implies that the repeatability of interactions in USC06 is stronger than that in FDU13.

The stationary density of infected individuals $\rho_I$ in the online-offline multiplex networks with three online social networks are almost the same for both FDU13 and USC06 (see Fig.6). Thus, we plot the differences of the stationary density of infected individuals in multiplex networks with different online social networks directly. Fig.7 and Fig.8 show the difference $\rho_I^{IR\&F+FS} - \rho_I^{Alltypes}$ (*i.e.* the stationary density of infected individuals in multiplex networks with online social network IR&F+FS minus that with online social network All types) and the difference $\rho_I^{Alltypes} - \rho_I^{IR\&F+S}$ (*i.e.* the stationary density of infected individuals in multiplex networks with online social network All types minus that with online social network IR&F+S), respectively, versus the effective epidemic spreading rate $\beta^U/\mu$ and the awareness spreading rate $\nu/\delta$. We observe that $\rho_I^{IR\&F+FS} - \rho_I^{Alltypes}$ and $\rho_I^{Alltypes} - \rho_I^{IR\&F+S}$ are always positive for both FDU13 and USC06. It means that, at the same effective epidemic spreading rate and awareness spreading rate, the epidemic prevalence in multiplex networks with different online social networks has $\rho_I^{IR\&F+FS} \geq \rho_I^{Alltypes} \geq \rho_I^{IR\&F+S}$. A higher infection fraction at the steady state implies that the suppression of infection by the awareness in the online social network is weaker. Hence, we could reduce the epidemic prevalence in multiplex social networks by increasing the friendships between strangers on the online social networks.

To verify the effect of the number of edges in the online social networks on our results, we fix the effective epidemic spreading rate $\beta^U/\mu = 0.5$, the awareness spreading rate $\nu/\delta = 0.2$, and study the influence of the edge selection probability $\eta$ on the stationary density of infected individuals $\rho_I$. As shown in Fig.9, the epidemic prevalence $\rho_I$ decreases with the increase of the edge selection probability $\eta$ in all datasets. The epidemic prevalence $\rho_I$ in multiplex networks with the online social network IR&F+FS is always the largest, and that with the online social network IR&F+S is the smallest. Our results

(a)

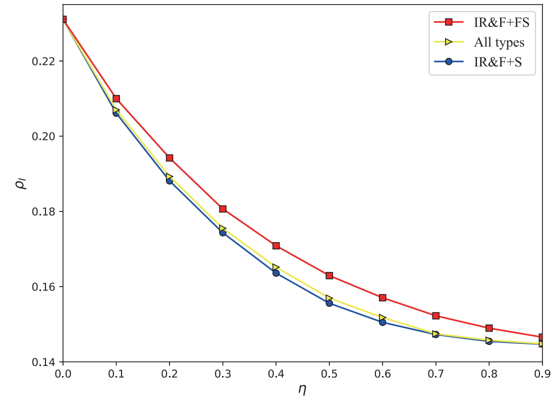


(b)

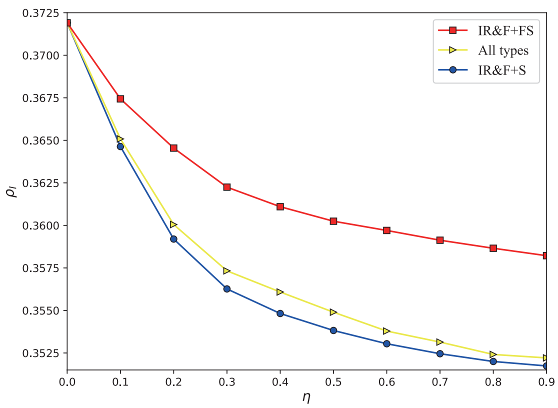


Fig. 9. The density of infected individuals at the steady state $\rho_I$ versus the edge selection probability $\eta$ in UAU-SIS dynamics with online-offline multiplex networks. (a), (b), (c) are simulated with FDU13; (d), (e), (f) are simulated with USC06. (a), (d) have the online social network IR&F+FS; (b), (e) have the online social network All types; (c), (f) have the online social network IR&F+S.

are confirmed to be independent of the number of edges in the online social networks.

## VI. Conclusion

Inspired by the real-world scenario, we study how social ties in online social network affect the epidemic spreading. We propose multiplex social network models with three different online social networks, *i.e.* IR&F+FS (consist of in-roles, friends and familiar strangers), All types (contain all four types of social ties) and IR&F+S (consist of in-roles, friends and strangers). We find that the epidemic prevalence increases with the effective epidemic spreading rate and decreases with the awareness spreading rate. The stationary density of infected individuals in multiplex networks with online social network IR&F+FS is the largest and that with online social network IR&F+S is the smallest, regardless the online social network density, the effective epidemic spreading rate and the awareness spreading rate in UAU-SIS dynamics. It is counterintuitive that the S social ties in online social networks are more likely to suppress the epidemic spreading than the FS social ties. Increasing the friendships between strangers in online social networks could reduce the epidemic prevalence in multiplex social networks. Our study provides a new perspective for friend recommendation systems in online social media to control epidemics.

## Acknowledgment

This work was supported in part by the National Natural Science Foundation of China (No.71731004, No.61603097), in part by the Natural Science Fund for distinguished Young Scholar of China (No. 61425019), in part by Natural Science Foundation of Shanghai (No.16ZR1446400).

## References

[1] Roy M Anderson, B Anderson, and Robert M May. *Infectious diseases of humans: dynamics and control*. Oxford university press, 1992.
[2] Cong Li, Ruud van de Bovenkamp, and Piet Van Mieghem. Susceptible-infected-susceptible model: A comparison of n-intertwined and heterogeneous mean-field approximations. *Physical Review E*, 86(2):026116, 2012.
[3] Faryad Darabi Sahneh, Caterina Scoglio, and Piet Van Mieghem. Generalized epidemic mean-field model for spreading processes over multilayer complex networks. *IEEE/ACM Transactions on Networking (TON)*, 21(5):1609–1620, 2013.
[4] Romualdo Pastor-Satorras, Claudio Castellano, Piet Van Mieghem, and Alessandro Vespignani. Epidemic processes in complex networks. *Reviews of modern physics*, 87(3):925, 2015.
[5] Romualdo Pastor-Satorras and Alessandro Vespignani. Epidemic spreading in scale-free networks. *Physical review letters*, 86(14):3200, 2001.
[6] Wei Wang, Quan-Hui Liu, Shi-Min Cai, Ming Tang, Lidia A Braunstein, and H Eugene Stanley. Suppressing disease spreading by using information diffusion on multiplex networks. *Scientific reports*, 6:29259, 2016.
[7] Sebastian Funk, Erez Gilad, Chris Watkins, and Vincent AA Jansen. The spread of awareness and its impact on epidemic outbreaks. *Proceedings of the National Academy of Sciences*, 106(16):6872–6877, 2009.
[8] Sebastian Funk, E Gilad, and Vincent AA Jansen. Endemic disease, awareness, and local behavioural response. *Journal of theoretical biology*, 264(2):501–509, 2010.
[9] Qingchu Wu, Xinchu Fu, Michael Small, and Xin-Jian Xu. The impact of awareness on epidemic spreading in networks. *Chaos: an interdisciplinary journal of nonlinear science*, 22(1):013101, 2012.
[10] Keith Paarporn, Ceyhun Eksin, Joshua S Weitz, and Jeff S Shamma. Networked sis epidemics with awareness. *IEEE Transactions on Computational Social Systems*, 4(3):93–103, 2017.
[11] Clara Granell, Sergio Gómez, and Alex Arenas. Dynamical interplay between awareness and epidemic spreading in multiplex networks. *Physical review letters*, 111(12):128701, 2013.
[12] Quantong Guo, Yanjun Lei, Xin Jiang, Yifang Ma, Guanying Huo, and Zhiming Zheng. Epidemic spreading with activity-driven awareness diffusion on multiplex network. *Chaos: An Interdisciplinary Journal of Nonlinear Science*, 26(4):043110, 2016.
[13] Nicola Perra, Bruno Gonçalves, Romualdo Pastor-Satorras, and Alessandro Vespignani. Activity driven modeling of time varying networks. *Scientific reports*, 2:469, 2012.
[14] Di Liang, Xiang Li, and Yi-Qing Zhang. Identifying familiar strangers in human encounter networks. *EPL (Europhysics Letters)*, 116(1):18006, 2016.
[15] Mark S Granovetter. The strength of weak ties. In *Social networks*, pages 347–367. Elsevier, 1977.
[16] Ronald S Burt. Structural holes and good ideas. *American journal of sociology*, 110(2):349–399, 2004.
[17] Simon Rodan and Charles Galunic. More than network structure: How knowledge heterogeneity influences managerial performance and innovativeness. *Strategic management journal*, 25(6):541–562, 2004.
[18] Márton Karsai, Nicola Perra, and Alessandro Vespignani. Time varying networks and the weakness of strong ties. *Scientific reports*, 4:4001, 2014.
[19] Brian Uzzi and Jarrett Spiro. Collaboration and creativity: The small world problem. *American journal of sociology*, 111(2):447–504, 2005.

[20] Elizabeth Long Lingo and Siobhán O'Mahony. Nexus work: Brokerage on creative projects. *Administrative science quarterly*, 55(1):47–81, 2010.

[21] Lynn Wu, Benjamin N Waber, Sinan Aral, Erik Brynjolfsson, and Alex Pentland. Mining face-to-face interaction networks using sociometric badges: Predicting productivity in an it configuration task. *Available at SSRN 1130251*, 2008.

[22] Stanley Milgram, John Ed Sabini, and Maury Ed Silver. *The individual in a social world: Essays and experiments*. Mcgraw-Hill Book Company, 1992.

[23] Eric Paulos and Elizabeth Goodman. The familiar stranger: anxiety, comfort, and play in public places. In *Proceedings of the SIGCHI conference on Human factors in computing systems*, pages 223–230. ACM, 2004.

[24] Lijun Sun, Kay W Axhausen, Der-Horng Lee, and Xianfeng Huang. Understanding metropolitan patterns of daily encounters. *Proceedings of the National Academy of Sciences*, 110(34):13774–13779, 2013.

[25] Nathan Eagle, Alex Sandy Pentland, and David Lazer. Inferring friendship network structure by using mobile phone data. *Proceedings of the national academy of sciences*, 106(36):15274–15278, 2009.

[26] Cong Li, Huijuan Wang, and Piet Van Mieghem. Epidemic threshold in directed networks. *Physical Review E*, 88(6):062802, 2013.

[27] Xiao-Jie Li, Cong Li, and Xiang Li. The impact of information dissemination on vaccination in multiplex networks. *arXiv preprint arXiv:1810.09439*, 2018.

[28] Yi-Qing Zhang, Xiang Li, Jian Xu, and Athanasios V Vasilakos. Human interactive patterns in temporal networks. *IEEE Transactions on Systems, Man, and Cybernetics: Systems*, 45(2):214–222, 2014.

[29] Wei-jen Hsu, Debojyoti Dutta, and Ahmed Helmy. Structural analysis of user association patterns in university campus wireless lans. *IEEE Transactions on Mobile Computing*, 11(11):1734–1748, 2011.

[30] Augustin Chaintreau, Pan Hui, Jon Crowcroft, Christophe Diot, Richard Gass, and James Scott. Impact of human mobility on opportunistic forwarding algorithms. *IEEE Transactions on Mobile Computing*, (6):606–620, 2007.

[31] Wei-Jen Hsu, Thrasyvoulos Spyropoulos, Konstantinos Psounis, and Ahmed Helmy. Modeling spatial and temporal dependencies of user mobility in wireless mobile networks. *IEEE/ACM Transactions on networking*, 17(5):1564–1577, 2009.

[32] Yi-Qing Zhang and Xiang Li. Temporal dynamics and impact of event interactions in cyber-social populations. *Chaos: An Interdisciplinary Journal of Nonlinear Science*, 23(1):013131, 2013.

[33] Cong Li, Shumin Zhang, and Xiang Li. Can multiple social ties help improve human location prediction? *Physica A: Statistical Mechanics and its Applications*, 525:1276–1288, 2019.

[34] Gjergji Zyba, Geoffrey M Voelker, Stratis Ioannidis, and Christophe Diot. Dissemination in opportunistic mobile ad-hoc networks: The power of the crowd. In *2011 Proceedings IEEE INFOCOM*, pages 1179–1187. IEEE, 2011.

[35] Dashun Wang, Dino Pedreschi, Chaoming Song, Fosca Giannotti, and Albert-Laszlo Barabasi. Human mobility, social ties, and link prediction. In *Proceedings of the 17th ACM SIGKDD international conference on Knowledge discovery and data mining*, pages 1100–1108. Acm, 2011.